

Supporting Information

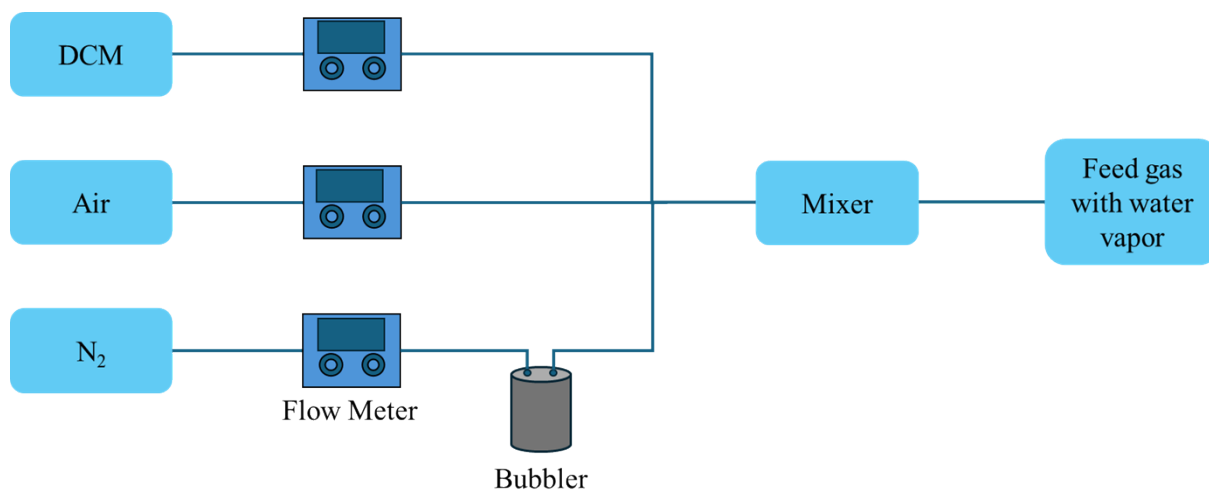
Improving photocatalytic activity and chlorine resistance performance of carbon nanolayer wrapped TiO₂ nanocomposite catalyst for dichloromethane purification

Hongli Liu,^{ab} Jinhua Feng,^{ab} Xin Wang,^{ab} Maosen Xu,^{ab} Yunzheng Deng,^{ab} Guiying Li,^{ab} Yingxin Yu,^{ab} Taicheng An^{*ab}

^a *Guangdong Key Laboratory of Environmental Catalysis and Health Risk Control, Guangdong-Hong Kong-Macao Joint Laboratory for Contaminants Exposure and Health, Institute of Environmental Health and Pollution control, Guangdong University of Technology, Guangzhou 510006, China.*

^b *Guangdong Engineering Technology Research Center for Photocatalytic Technology Integration and Equipment, Guangdong Basic Research Center of Excellence for Ecological Security and Green Development, School of Environmental Science and Engineering, Guangdong University of Technology, Guangzhou 510006, China.*

*** Corresponding author: Prof. Taicheng An, E-mail: antc99@gdut.edu.cn**



Scheme S1. Preparation diagram for the feed gas with water vapor.

For the preparation of the feed gas used in water resistance test, N₂ gas through a bubbler containing water at a certain flow rate, in which the bubbler's temperature is stabilized at 30 °C by a thermostatic water bath. Then the N₂ gas with water vapor is mixed with dry air and the standard gas of DCM diluted with N₂ to obtain the feed gas with 70 ± 1 ppmv of DCM and 10 vol % water vapor.

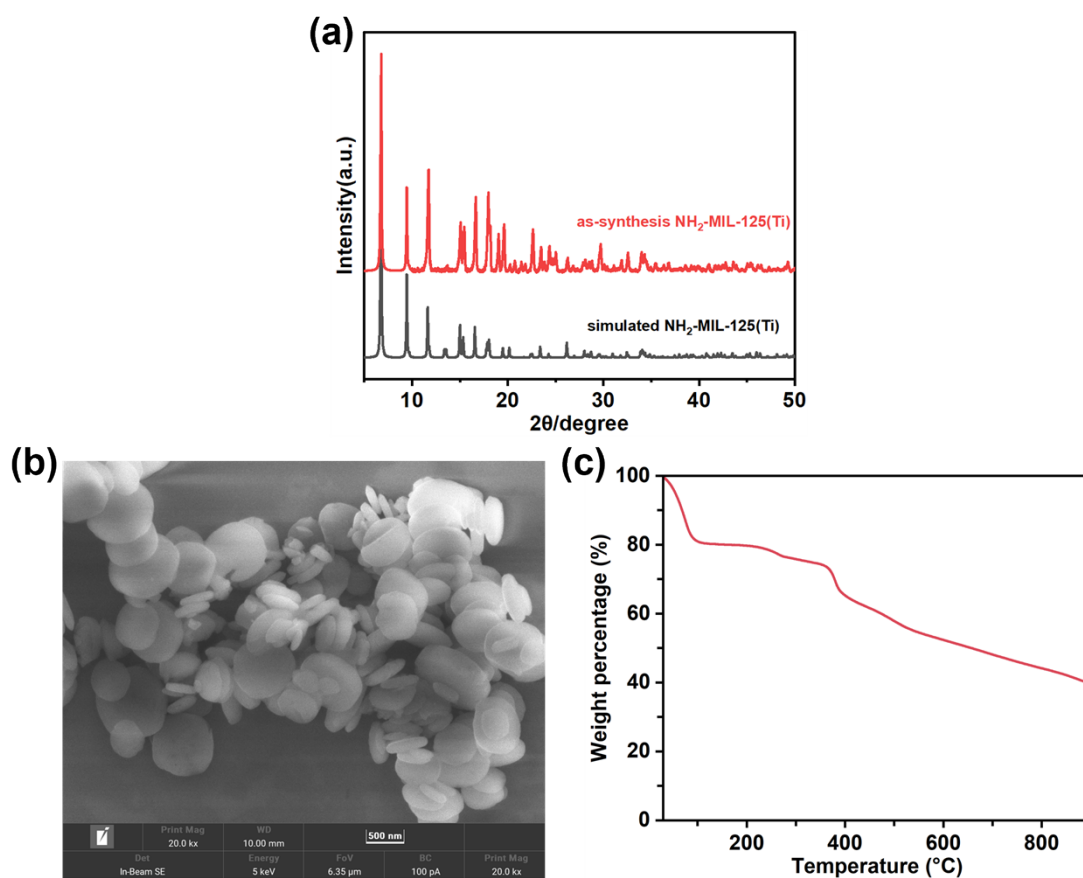


Figure S1. (a) Powder XRD patterns of the simulated and as-synthesized NH₂-MIL-125, (b) SEM image and (c) TGA spectra of as-synthesized NH₂-MIL-125.

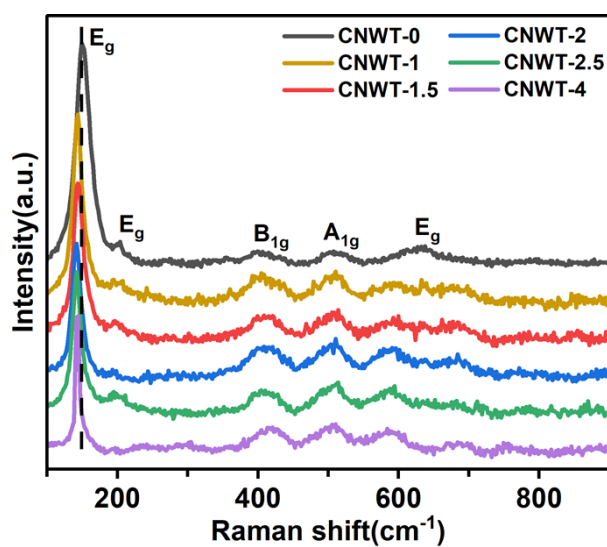


Figure S2. Raman spectra of the CNWT-0 and CNWT-x samples.

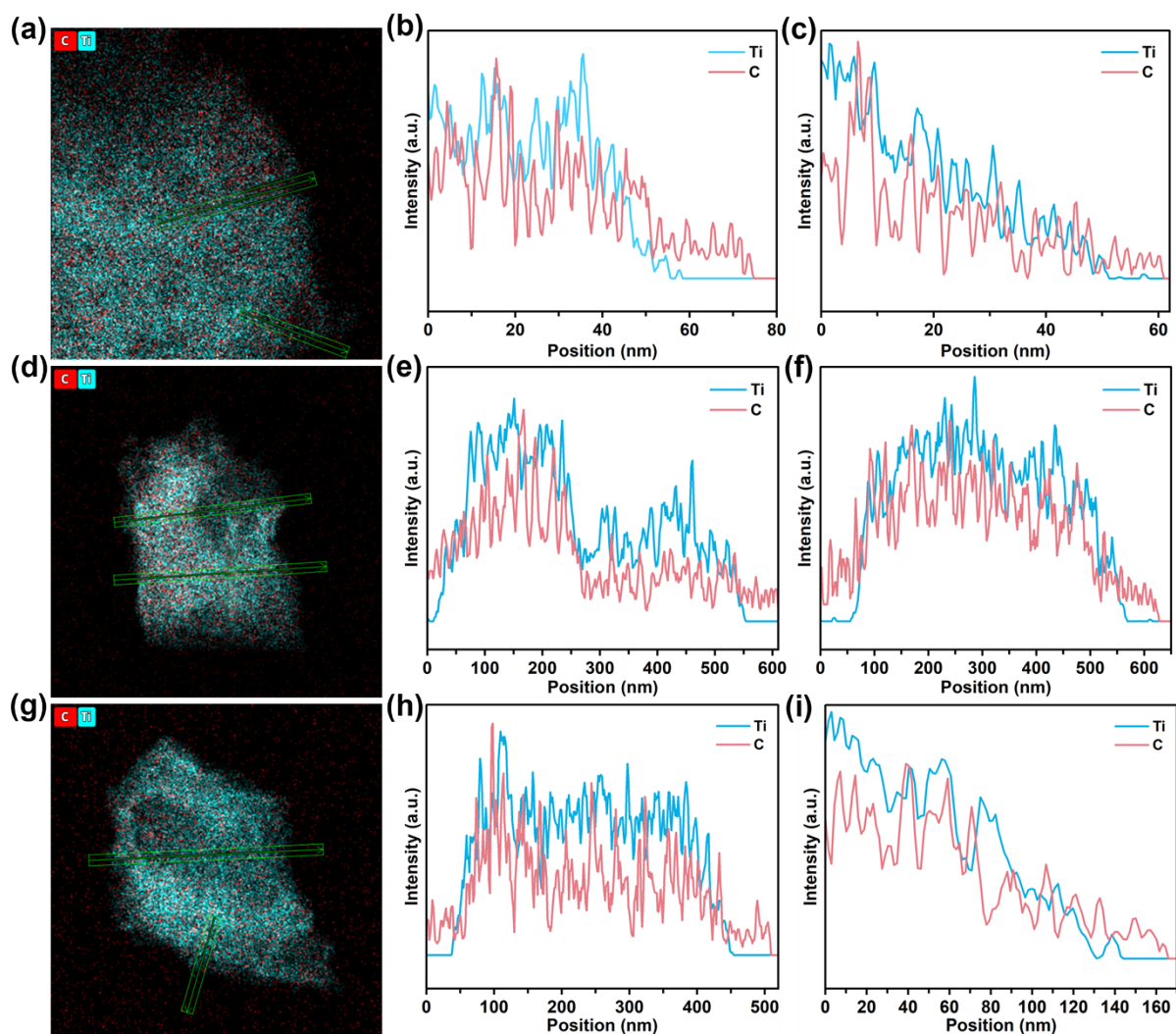


Figure S3. The elemental line scans of the CNWT-0 (a-f) and CNWT-2 (g-i) samples.

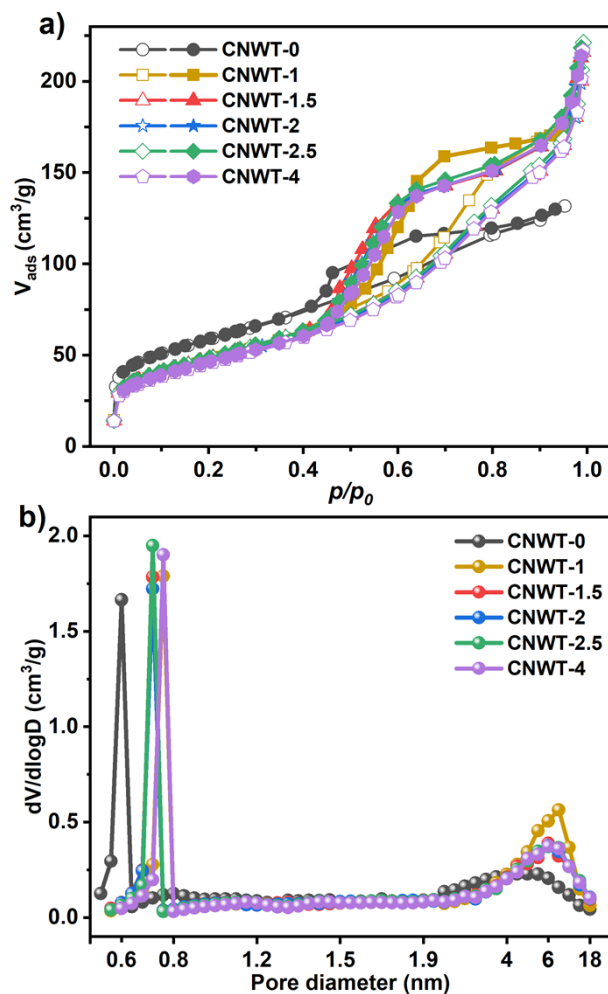


Figure S4. N_2 adsorption-desorption isotherms (a) and pore size distribution (b) of the CNWT-0 and CNWT-x samples.

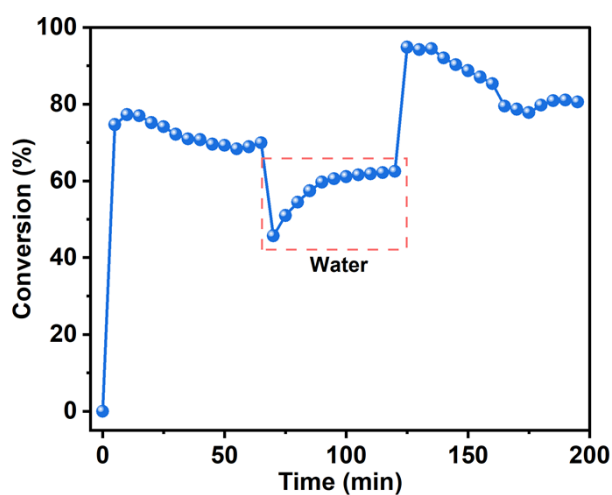


Figure S5. The DCM conversion over CNWT-2 under 10 vol % of water vapor condition.

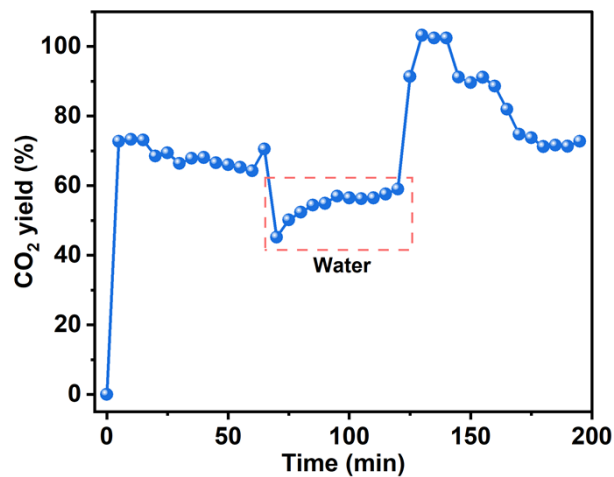


Figure S6. The CO₂ yield during the photocatalytic oxidation of DCM over CNWT-2 under 10 vol % of water vapor condition.

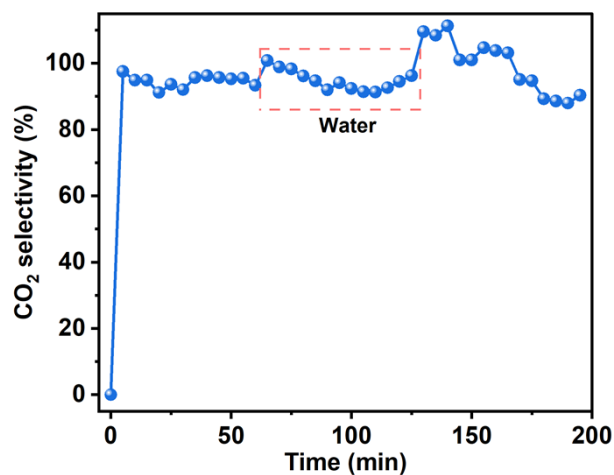


Figure S7. The CO₂ selectivity during the photocatalytic oxidation of DCM over CNWT-2 under 10 vol % of water vapor condition.

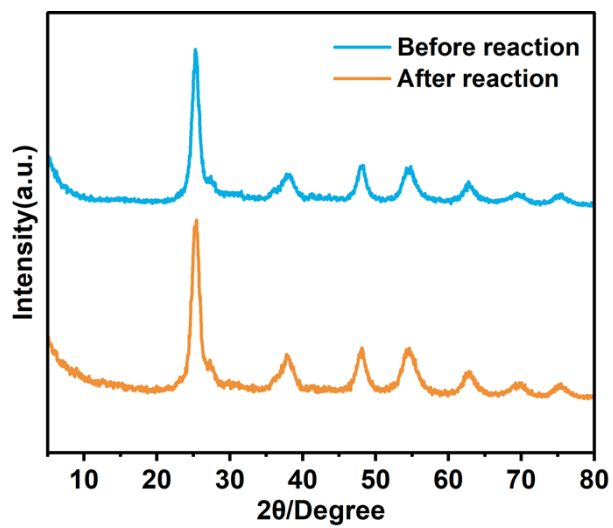


Figure S8. XRD patterns of the CNWT-2 sample before and after the catalytic reaction.

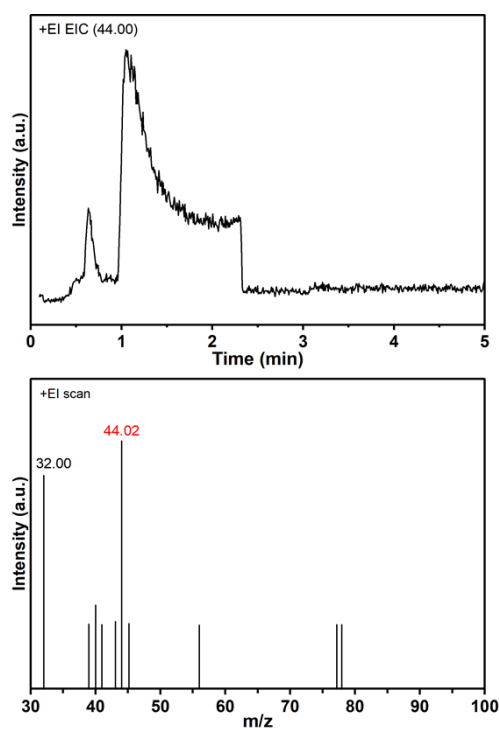


Figure S9. GC-MS spectra of CO₂ in the exit gas.

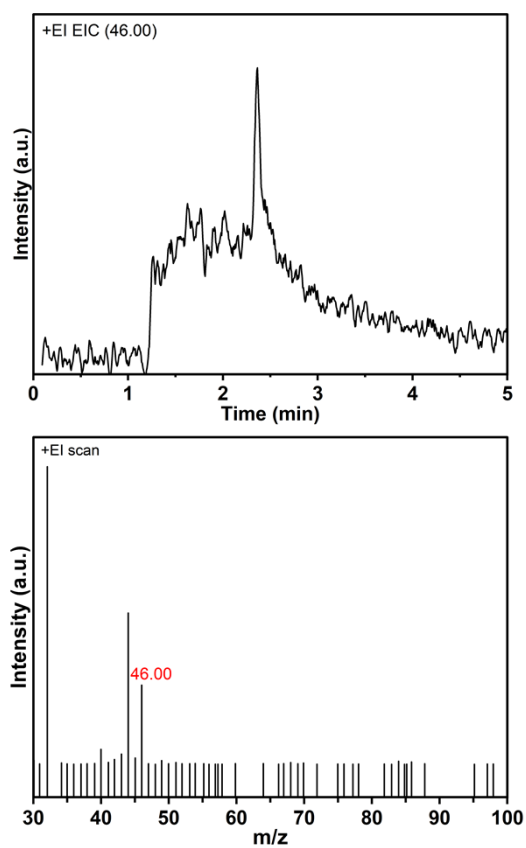


Figure S10. GC-MS spectra of HCOOH in the exit gas.

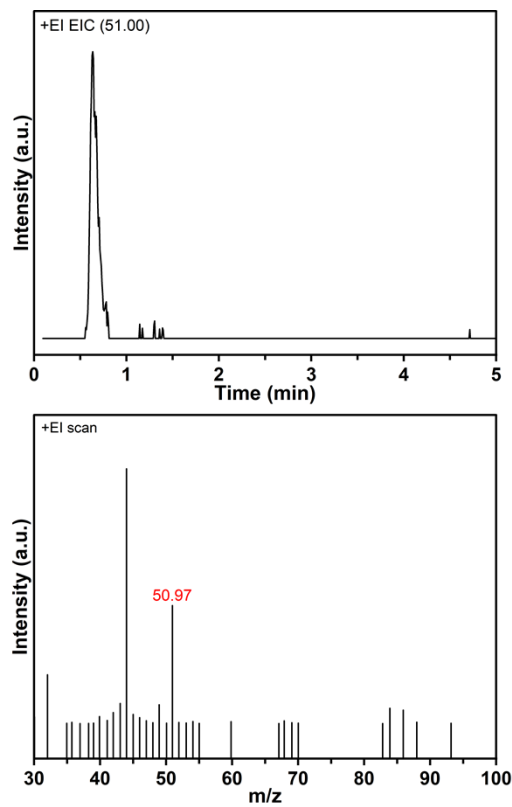


Figure S11. GC-MS spectra of CH_3Cl in the exit gas.

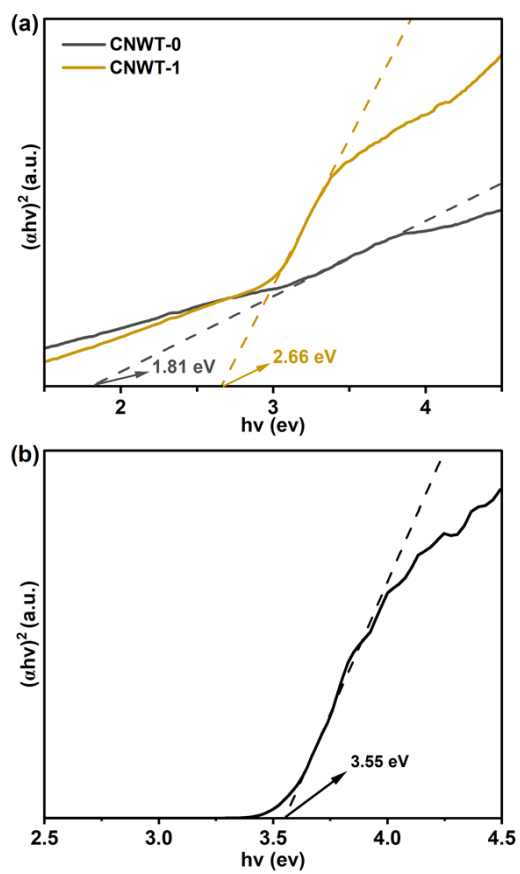


Figure S12. Band gap spectra of CNWT-0, CNWT-1 samples(a) and commercial P25 TiO_2 (b).

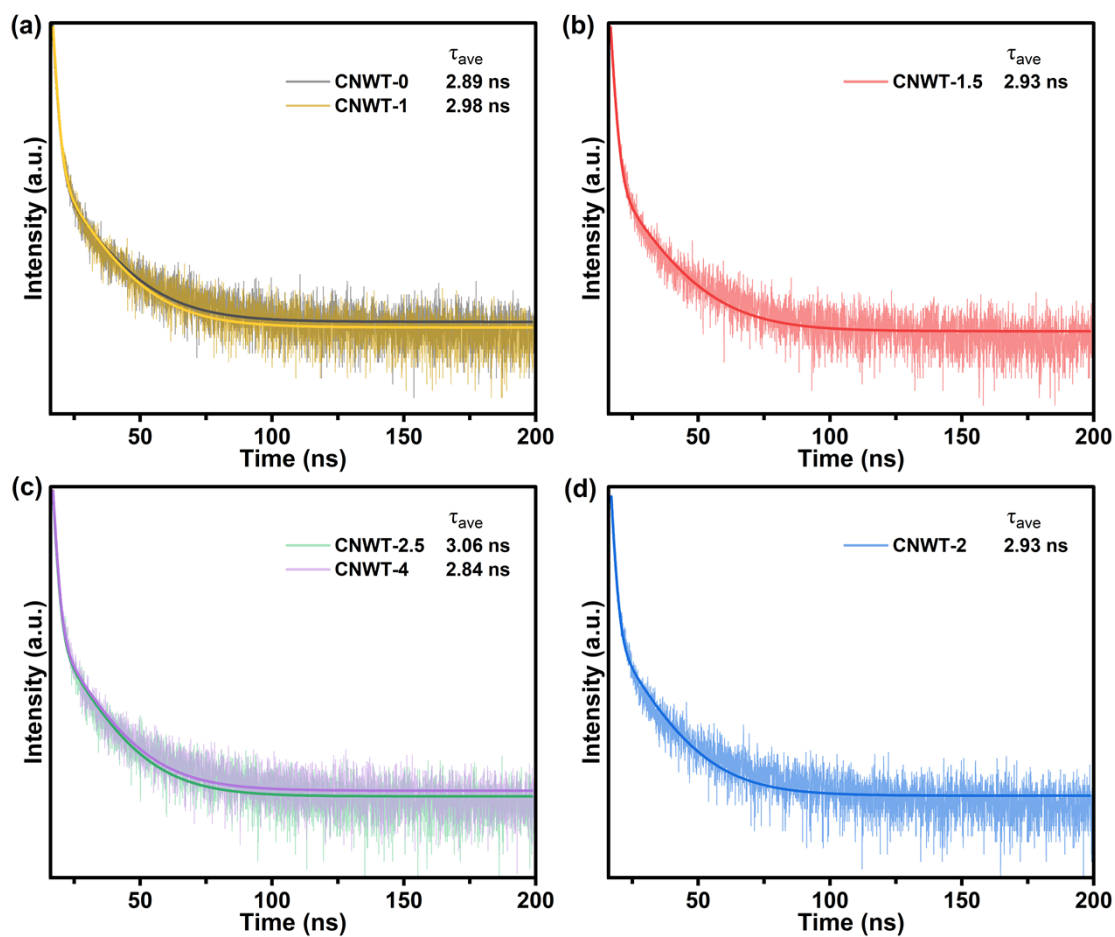


Figure S13. Time-resolved photoluminescence spectra of the CNWT-0 and CNWT-x samples.

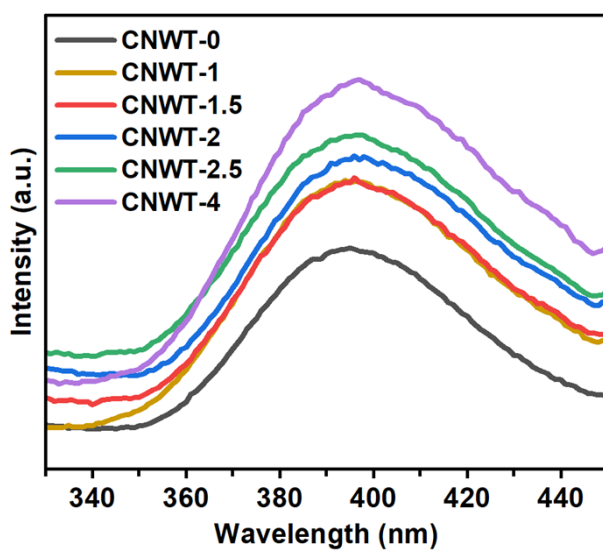


Figure S14. Steady-state fluorescence spectra of the CNWT-0 and CNWT-x samples.

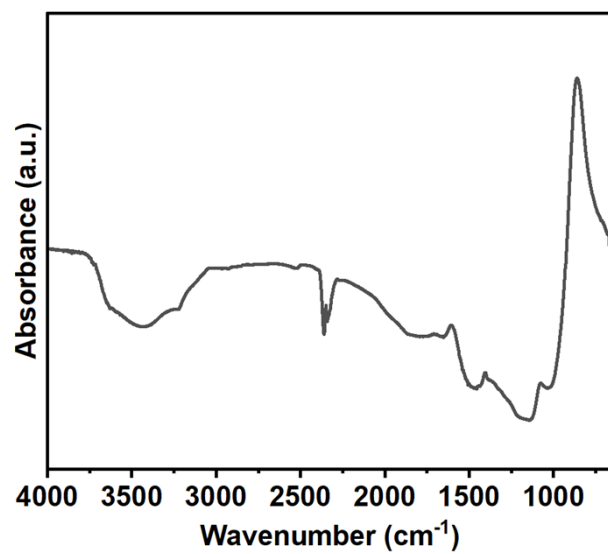


Figure S15. IR spectra of CNWT-2.

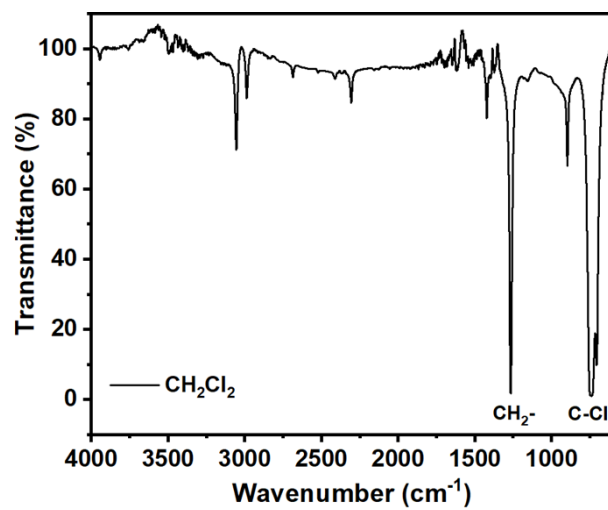


Figure S16. IR spectra of CH₂Cl₂.

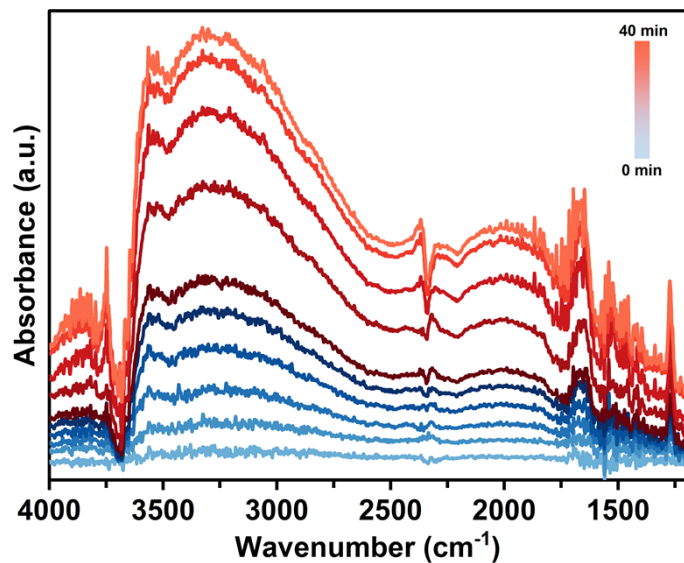


Figure S17. *In-situ* DRIFTS spectra of DCM adsorbed onto the CNWT-2 sample in the 4000-1200 cm^{-1} range.

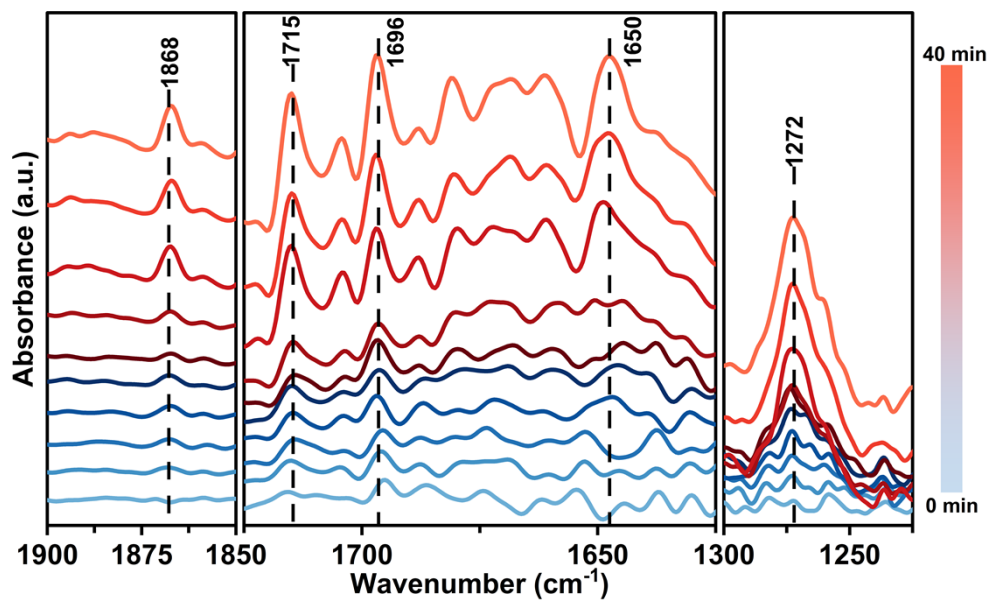


Figure S18. *In-situ* DRIFTS spectra of DCM adsorbed onto the CNWT-2 sample in the 1900-1200 cm^{-1} range.

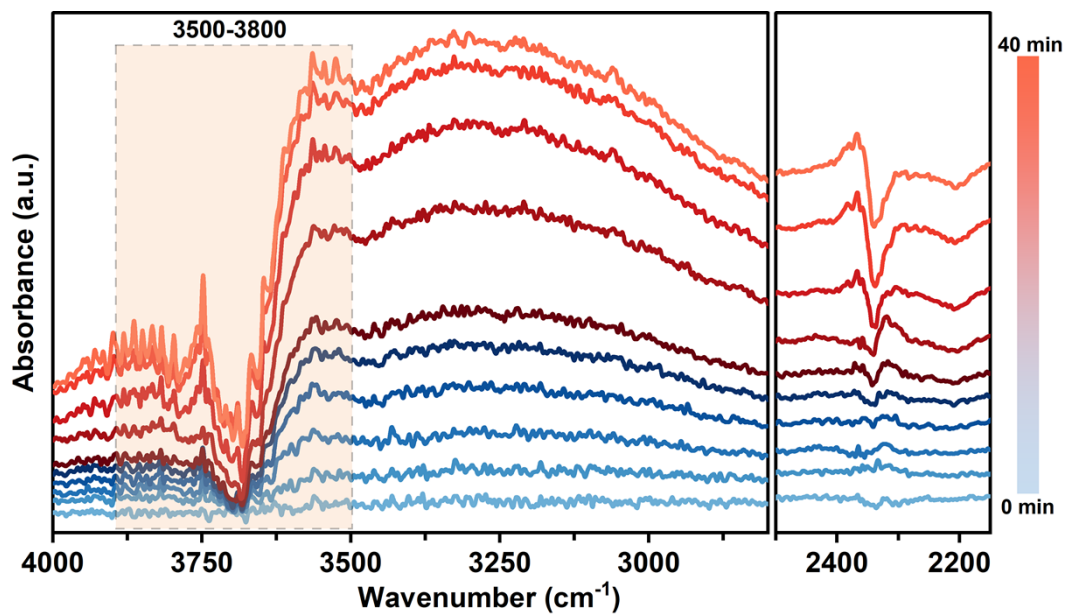


Figure S19. *In-situ* DRIFTS spectra of DCM adsorbed onto the CNWT-2 sample in the 4000-2100 cm^{-1} range.

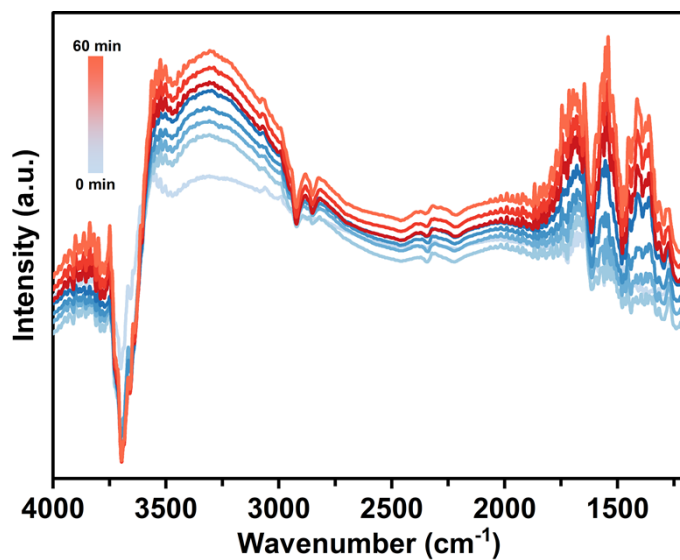


Figure S20. *In-situ* DRIFTS spectra of DCM photocatalytic oxidation as a function of time over CNWT-2 under UV-vis light irradiation.

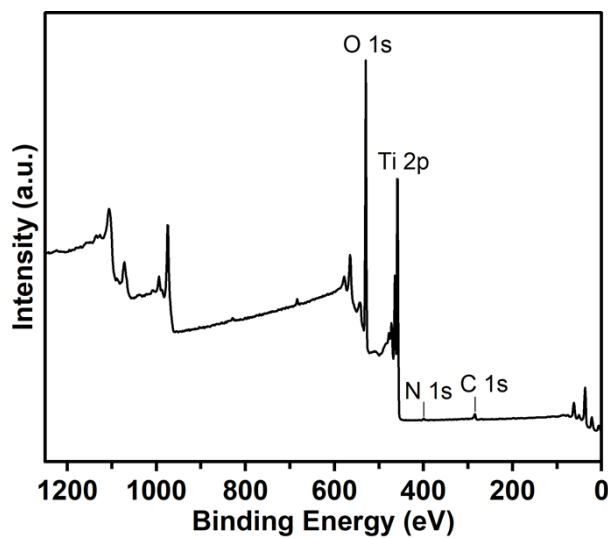


Figure S21. The *in-situ* NAP XPS survey spectra of the fresh CNWT-2 sample.

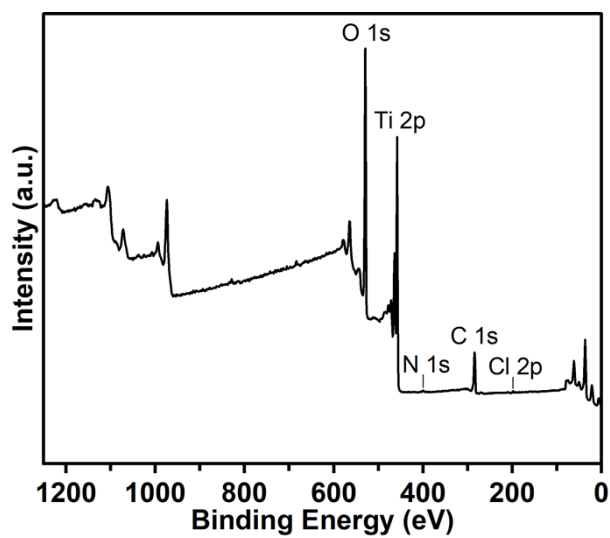


Figure S22. The *in-situ* NAP XPS survey spectra of CNWT-2 in air-balanced DCM conditions without light irradiation.

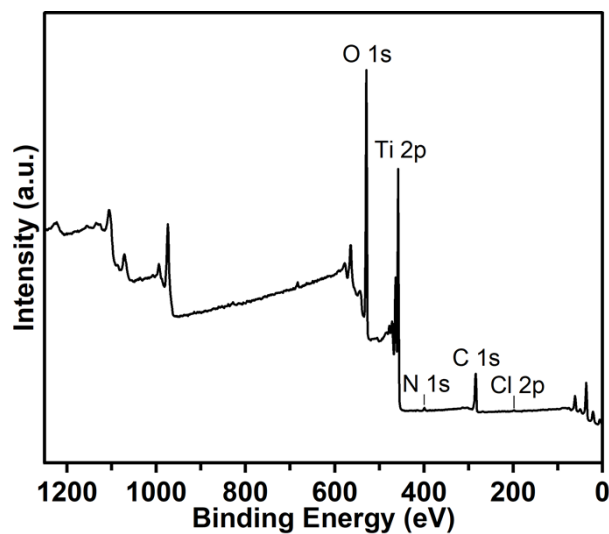


Figure S23. The *in-situ* NAP XPS survey spectra of CNWT-2 in air-balanced DCM conditions under UV-vis light irradiation.

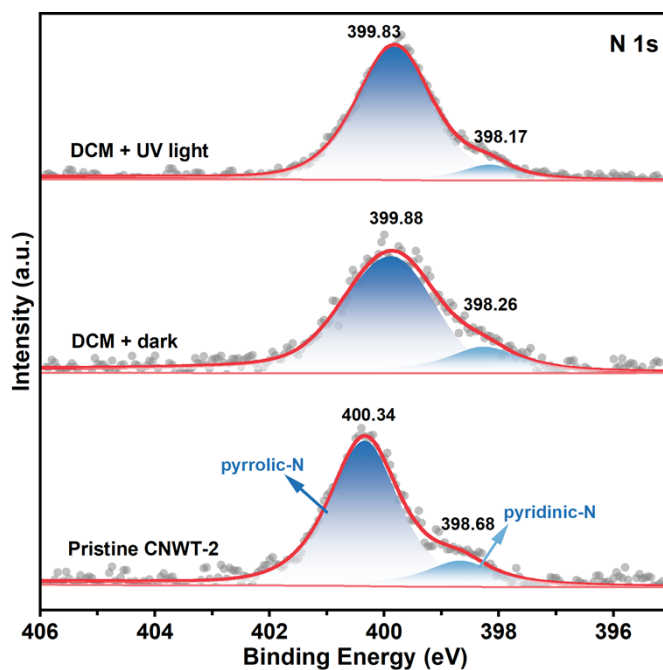


Figure S24. *In-situ* NAP XPS spectra of N 1s for the CNWT-2 sample.

Table S1. The relative ratio of D band to G band (I_D/I_G) and the carbon content of CNWT-0 and CNWT-x samples.

Sample	CNWT-0	CNWT-1	CNWT-1.5	CNWT-2	CNWT-2.5	CNWT-4
I_D/I_G	0.85	0.83	0.87	0.85	1.05	1.01
C (%)	42.33	32.45	29.03	23.07	18.12	16.08

Table S2. The specific surface area and porosity of the CNWT-0 and CNWT-x samples.

Sample	S_{BET} (m ² /g)	V_p (cm ³ /g)	D_p (nm)
CNWT-0	204.47	0.20	3.98
CNWT-1	170.1	0.27	6.28
CNWT-1.5	171.97	0.33	7.60
CNWT-2	170.43	0.33	7.71
CNWT-2.5	171.91	0.33	7.63
CNWT-4	163.91	0.32	7.95

Table S3. Fitting parameters for Time-resolved photoluminescence of the CNWT-0 and CNWT-x samples.

Sample	A_1	τ_1	A_2	τ_2	τ_{ave}
CNWT-0	40813.55	1.57	0.39	16.38	2.89
CNWT-1	60617.12	1.52	0.45	15.71	2.98
CNWT-1.5	35807.81	1.58	0.38	16.57	2.93
CNWT-2	0.46	15.26	134192.80	1.42	2.93
CNWT-2.5	0.47	15.00	106546.00	1.44	3.06
CNWT-4	0.47	15.21	95174.71	1.46	2.84